Study of Film Structure and Adsorption Kinetics of Polyelectrolyte Multilayer Films: Effect of pH and Polymer Concentration

Akhilesh Garg,[†] James R. Heflin,[‡] Harry W. Gibson,[§] and Richey M. Davis*[,†]

Departments of Chemical Engineering, Physics, and Chemistry, Virginia Tech, Blacksburg, Virginia 24061

Received February 15, 2008. Revised Manuscript Received July 7, 2008

The alternate adsorption of polycation poly(allylamine hydrochloride)(PAH) and the sodium salt of the polymeric dye poly{1-[*p*-(3′-carboxy-4′-hydroxyphenylazo)benzenesulfonamido]-1,2-ethandiyl}(PCBS) on quartz crystals coated with silica was studied to understand the structural properties and adsorption kinetics of these films using a combination of quartz crystal microbalance with dissipation monitoring (QCM-D), absorbance, and ellipsometry measurements. In-situ deposition of the polycation PAH on QCM crystals was monitored, followed by rinsing with water and then deposition of the polyanion PCBS. The effects of polymer concentration and pH on film structure, composition and adsorption kinetics were probed. The polymers were adsorbed at neutral pH conditions and at elevated pH conditions where PAH was essentially uncharged to obtain much thicker films. The change in the resonant frequency, Δf, of the QCM-D showed a linear decrease with the number of bilayers, a finding consistent with absorbance and ellipsometric thickness measurements which showed linear growth of film thickness. By using the Δf ratios of PCBS to PAH, the molar ratios of repeat units of PCBS to PAH in the bilayer films as determined by QCM-D were ∼1:1 at polyelectrolyte concentrations 5−10 mM repeat unit, indicating complete dissociation of the ionic groups. The frequency and dissipation data from the QCM-D experiments were analyzed with the Voigt model to estimate the thickness of the hydrated films which were then compared with thicknesses of dry films measured by ellipsometry. This led to estimates of the water content of the films to be ∼45 wt %. In addition to the QCM-D, some films were also characterized by a QCM which measures only the first harmonic without dissipation monitoring. For the deposition conditions studied, the deposited mass values measured by the QCM's first harmonic were similar to the results obtained using higher harmonics from QCM-D, indicating that the self-assembled polyelectrolyte films were rigid.

Introduction

Organic materials are of great interest as active components in electronic devices due to the ease with which their properties can be tuned at the molecular level and their ease of fabrication. Thin films of organic materials are particularly interesting for applications in light-emitting diodes, photovoltaics, electrochromic devices, electro-optic modulators, integrated molecular optics, biosensors, and fuel cells.[1−4] One of the methods for fabrication of organic thin films involves the alternate adsorption of polycations and polyanions on a charged surface which leads to the formation of ionic self-assembled multilayer (ISAM) films, also commonly referred to as layer-by-layer (LbL) films.[5,6] When a polyelectrolyte adsorbs onto an oppositely charged surface, charge reversal on the surface typically occurs; this facilitates the adsorption of the next layer of oppositely charged polymer. In principle, films with an arbitrary number of bilayers can be fabricated in this fashion. Rational applications of this technique require an understanding of the internal architecture of these films, such as composition, structure and mechanical properties[7] and an understanding of how solution parameters such as concentration and pH affects the internal structure of these films.[8−11]

Our work involves the study of ISAM films at the molecular level to understand the composition of these films which exhibit nonlinear optical (NLO) effects due to inclusion of an NLO chromophore that can be oriented in a polar manner.[12−18] Films exhibiting NLO effects have applications in electro-optic (EO) modulators which convert electrical signals to optical signals and thus play an important role in communication networks. In organic films, the second order nonlinear susceptibility of an NLO film, $x^{(2)}$ is given by[19]

$$\chi^{(2)} = NF\beta\langle\cos^3\bar{\psi}\rangle \quad (1)$$

where N is the chromophore density, F is the local field factor which is a function of the refractive index, β is the hyperpolarizability, and $\bar{\psi}$ is the orientation angle of the chromophores.

* To whom correspondence should be addressed. E-mail: rmdavis@vt.edu. Phone 1-540-231-4578. Fax 1-540-231-5022.

[†] Department of Chemical Engineering.

[‡] Department of Physics.

[§] Department of Chemistry.

(1) Fendler, J. H., Ed.; *Nanoparticles and Nanostructured Films: Preparation, Characterization and Applications*; Wiley-VCH: Weinheim, 1998.

(2) Lutkenhaus, J. L.; Hammond, P. T. *Soft Matter* **2007**, *3*, 804–816.

(3) Bertrand, P.; Jonas, A.; Laschewsky, A.; Legras, R. *Macromol. Rapid Commun.* **2000**, *21*, 319–348.

(4) Hammond, P. T. *Curr. Opin. Colloid Interface Sci.* **2000**, *4*, 430–442.

(5) Decher, G.; Hong, J. D. *Makromol. Chem., Makromol Symp.* **1991**, *46*, 321–327.

(6) Decher, G. *Science* **1997**, *277*, 1232–1237.

(7) Mermut, O.; Lefebvre, J.; Gray, D. G.; Barrett, C. J. *Macromolecules* **2003**, *36*, 8819–8824.

(8) Mermut, O.; Barrett, C. J. *J. Phys. Chem. B* **2003**, *107*, 2525–2530.

(9) Shiratori, S. S.; Rubner, M. F. *Macromolecules* **2000**, *33*, 4213–4219.

(10) Schlenoff, J. B.; Dubas, S. T. *Macromolecules* **2001**, *34*, 592–598.

(11) Lvov, Y.; Ariga, K.; Onda, M.; Ichinose, I.; Kunitake, T. *Langmuir* **1997**, *13*, 6195–6203.

(12) Heflin, J. R.; Figura, C.; Marciu, D. *Appl. Phys. Lett.* **1999**, *74*, 495–497.

(13) Heflin, J. R.; Guzy, M. T.; Neyman, P. J.; Gaskins, K. J.; Brands, C.; Wang, Z.; Gibson, H. W.; Davis, R. M.; Cott, K. E. V. *Langmuir* **2006**, *22*, 5723–5727.

(14) Van Cott, K.; Guzy, M.; Neyman, P.; Brands, C.; Heflin, J.; Gibson, H.; Davis, R. *Angew. Chem., Int. Ed.* **2002**, *41*, 3236–3238.

(15) Wang, X.; Balasubramanian, S.; Li, L.; Jiang, X.; Sandman, D. J.; Rubner, M. F.; Kumar, J. T. *Macromol. Rapid Commun.* **1997**, *18*, 451–459.

(16) Laschewsky, A.; Wischerhoff, E.; Kauranen, M.; Persoons, A. *Macromolecules* **1997**, *30*, 8304–8309.

(17) Roberts, M. J.; Lindsay, G. A.; Herman, W. N.; Wynne, K. J. *J. Am. Chem. Soc.* **1998**, *120*, 11202–11203.

(18) Lvov, Y.; Yamada, S.; Kunitake, T. *Thin Solid Films* **1997**, *300*, 107–112.

(19) Dalton, L. R.; Harper, A. W.; Ghosn, R.; Steier, W. H.; Ziari, M.; Fetterman, H.; Shi, Y.; Mustacich, R. V.; Jen, A. K.-Y.; Shea, K. J. *Chem. Mater.* **1995**, *7*, 1060–1081.

10.1021/la8005053 CCC: $40.75
Published on Web 09/12/2008

Rational design of NLO films thus involves choosing a chromophore with a suitably high β and incorporating it into a film with high density N and low tilt angle $\bar{\psi}$. In this paper, we probe how processing conditions for film formation affect N and the bilayer thickness.

There are many studies of ISAM films and their structural properties, but relatively few of films that exhibit significant second order NLO properties.[18,20] A study of structural and mechanical properties of NLO-active polyelectrolyte multilayer films was done by Mermut et al.;[7] however, NLO properties were not studied. Other studies to understand the structural properties of ISAM films have employed techniques such as surface plasmon resonance (SPR),[21,22] reflectometry,[23] in situ atomic force microscopy,[24] streaming potential measurements,[25] X-ray photoelectron spectroscopy (XPS),[21] ellipsometry and absorbance measurements,[8] quartz crystal microbalance (QCM),[18,21,26−32] and QCM-D.[22,33−38]

QCM, which measures the change in the fundamental resonant frequency of a piezoelectric crystal due to deposition, has been widely used in biosensors,[27,28,30,32] to study the adsorption of proteins,[39,40] to study adsorption of inorganic materials such as nanoparticles,[11,29] for measuring thin film growth in deposition and sputtering processes,[41] to measure changes in viscosity,[42] and to study polymer adsorption[31,37] and ISAM formation.[21,22,26−30,32,35,36,43] The more recent technique known as QCM-D can measure up to seven harmonics and their corresponding dissipations, which can provide additional information about the viscoelastic properties of attached films.[33,34,44,45]

Chart 1. Structure of PAH

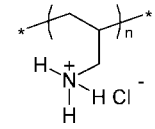

ISAM film formation has been studied with QCM, including the polycation:polyanion molar ratio in films as a function of pH,[43] the effect of varying polycation structure and concentration in combination with poly(sodium 4-styrenesulfonate) (PSS),[26] and the effect of solvent quality on film morphology and the kinetics of film growth.[46] ISAM formation involving the azobenzene-containing polyanion (PAZO, also known as PCBS, the polyanion used in the present study) has been studied using QCM as well. In-situ adsorption measurements of films composed of poly(dimethyldiallylammonium chloride)(PDDA) and PCBS revealed that the PCBS/PDDA mass ratio was ∼1:2 corresponding to a PCBS:PDDA molar ratio of 1:4.[18] While the frequency shift showed a linear growth with the number of bilayers, second harmonic generation (SHG) measurements did not show a quadratic increase with the number of bilayers, indicating that the polar orientation of the chromophores was not maintained as the number of bilayers increased. ISAM formation involving PCBS was also studied using PDDA and poly(ethyleneimine) in which QCM studies of dried films revealed that PCBS adsorbed onto PEI as aggregates, whereas it did not aggregate when adsorbing onto PDDA. However, NLO properties of the films were not studied.[32]

The present study demonstrates a methodology that combines in situ QCM-D measurements of hydrated films with absorbance and ellipsometry measurements to probe the effect of polymer concentration and pH on the polyanion/polycation ratio, the water content, and the structure of ISAM films. The conditions of polymer concentration and pH were chosen to complement a companion study of the NLO properties of PCBS/PAH ISAM films.[20] In that study, we found that films deposited at pH 7 where the PAH was highly charged were optically homogeneous and exhibited long-range polar ordering of the azobenzene chromophore in PCBS for films consisting of more than 600 bilayers. When the PAH was deposited at pH 9 where it was partly charged, the bilayer thickness was greater than for the pH 7 case, but long-range polar ordering disappeared after 200 bilayers. The reason why PAH results in polar orientation of the PCBS chromophore, while PDDA does not in films with bilayer numbers $>10-20$ is still an open question, leading to a need for a more detailed study of the formation of ISAM films containing PCBS; particularly we sought to delineate those conditions that lead to homogeneous film formation at high bilayer numbers. In the present study for selected deposition conditions, we compare analyses of films using both QCM-D and QCM and also study the kinetics of multilayer formation.

Experimental Section

Materials. Poly(allylamine hydrochloride)(PAH, Chart 1) was used as the polycation (M_w ca. 70 kDa; Aldrich). Poly{1-[*p*-(3′-carboxy-4′-hydroxyphenylazo)benzenesulfonamido]-1,2-ethandiyl}(Aldrich, PCBS, Chart 2) was used as the polyanionic chromophore. PCBS has an azobenzene side group that has a sufficiently high hyperpolarizability, β, to give a measurable SHG signal. Deionized (DI) water (Barnstead ROpureST; model no. D6311) with a resistivity >17 MΩ·cm was used. The ionic strength of the polymer solutions was adjusted using sodium chloride (Fisher

(20) Garg, A.; Durak, C.; Heflin, J. R.; Gibson, H. W.; Davis, R. M. *J. Appl. Phys.* Accepted.
(21) Caruso, F.; Niikura, K.; Furlong, D. N.; Okahata, Y. *Langmuir* **1997**, *13*, 3422–3426.
(22) Quinn, J. F.; Yeo, J. C. C.; Caruso, F. *Macromolecules* **2004**, *37*, 6537–6543.
(23) Kovacevic, D.; Burgh, S. v. d.; Keizer, A. d.; Stuart, M. A. C *Langmuir* **2002**, *18*, 5607–5612.
(24) Lavalle, P.; Gergely, C.; Cuisinie, F. J. G.; Decher, G.; Schaaf, P.; Voegel, J. C.; Picart, C. *Macromolecules* **2002**, *11*, 4458–4465.
(25) Dijt, J. C.; Stuart, M. A. C.; Fleer, G. J. *Macromolecules* **1992**, *25*, 5416–5423.
(26) Baba, A.; Kaneko, F.; Advincula, R. C. *Colloids Surf., A* **2000**, *173*, 39–49.
(27) ki, M. S.; Loikas, K.; Kankare, J. *Anal. Chem.* **2003**, *75*, 5895–5904.
(28) Ariga, K.; Lvov, Y.; Kunitake, T. *J. Am. Chem. Soc.* **1997**, *119*, 2224–2231.
(29) Ariga, K.; Lvov, Y.; Ichinose, I.; Kunitake, T. *Appl. Clay Sci.* **1999**, *15*, 137–152.
(30) Schoeler, B.; Poptoshev, E.; Caruso, F. *Macromolecules* **2003**, *36*, 5258–5264.
(31) Park, M.-K.; Youk, J. H.; Pispas, S.; Hadjichristidis, N.; Advincula, R. *Langmuir* **2002**, *18*, 8040–8044.
(32) Dante, S.; Advincula, R.; Frank, C. W.; Stroeve, P. *Langmuir* **1999**, *15*, 193–201.
(33) Voinova, M. V.; Rodahl, M.; Jonson, M.; Kasemo, B. *Phys. Scr.* **1999**, *59*, 391–396.
(34) Rodahl, M.; Kasemo, B. *Sensors Actuators A* **1996**, *54*, 448–456.
(35) Vogt, B. D.; Lin, E. K.; Wu, W.-l.; White, C. C *J. Phys. Chem. B* **2004**, *108*, 12685–12690.
(36) Norgren, M.; Gardlund, L.; Notley, S. M.; Htun, M.; Wågberg, L. *Langmuir* **2007**, *23*, 3737–3743.
(37) Munro, J. C.; Frank, C. W. *Macromolecules* **2004**, *37*, 925–938.
(38) Hubsch, E.; Ball, V.; Senger, B.; Decher, G.; Voegel, J.-C.; Schaaf, P. *Langmuir* **2004**, *20*, 1980–1985.
(39) Marxer, C. G.; Coen, M. C.; Schlapbach, L. *J. Colloid Interface Sci.* **2003**, *261*, 291–298.
(40) Hook, F.; Voros, J.; Rodahl, M.; Kurrat, R.; Boni, P.; Ramsden, J. J.; Textor, M.; Spencer, N. D.; Tengvall, P. J; Gold, B. K. *Colloids Surf., B* **2002**, *24*, 155–170.
(41) Bouzidi, L.; Narine, S. S.; Stefanov, K. G.; Slavina, A. J. *Rev. Sci. Instrum.* **2003**, *74*, 3039–3044.
(42) Gee, W. A.; Ritalahti, K. M.; Hunt, W. D.; Löffler, F. E. *IEEE Sensors J.* **2003**, *3*, 304–309.
(43) Lvov, Y.; Ariga, K.; Onda, M.; Ichinose, I.; Kunitake, T. *Colloids Surf., A* **1999**, *146*, 337–346.
(44) de Kerchove, A. J.; Elimelech, M. *Macromolecules* **2006**, *39*, 6558–6564.
(45) de Kerchove, A. J.; Elimelech, M. *Biomacromolecules* **2007**, *8*, 113–121.
(46) Poptoshev, E.; Schoeler, B.; Caruso, F. *Langmuir* **2004**, *20*, 829–834.

Chart 2. Structure of PCBS

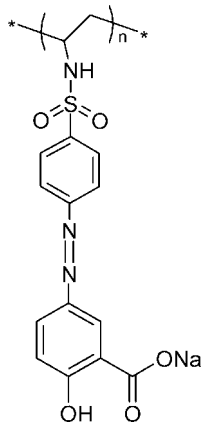

Table 1. Deposition Conditions Studied Using QCM-D, Absorbance and Ellipsometry Measurements

deposition condition	PAH repeat unit concn (mM)	PCBS repeat unit concn (mM)	pH_{PAH}	pH_{PCBS}
1 $(PAH\text{-}1/PCBS\text{-}1)_{7/7}$	1.0	1.0	7	7
2 $(PAH\text{-}5/PCBS\text{-}5)_{7/7}$	5.0	5.0	7	7
3 $(PAH\text{-}10/PCBS\text{-}10)_{7/7}$	10.0	10.0	7	7
4 $(PAH\text{-}10/PCBS\text{-}10)_{9/8}$	10.0	10.0	9	8

Scientific). The pHs of the polymer solutions were adjusted using 1.0 or 0.1 M solutions of sodium hydroxide and hydrogen chloride.

Absorbance and Ellipsometry. Absorbance measurements were done using a Perkin-Elmer Lambda 25 UV/vis system. The films exhibited an absorbance maximum, λ_{max}, at 360 nm, due to absorption by PCBS. Film thicknesses were measured using a variable angle spectroscopic ellipsometer (J.A. Woolam ellipsometer VB-200 with WVASE32 software version 3.361). Both absorbance and ellipsometry measurements were done on films fabricated on a glass substrate, the details of which can be found in a companion study.[20] Details of the ellipsometry procedure are found in the Supporting Information.

Quartz Crystal Microbalance. Two different quartz crystal microbalances were used in this study—a QCM-D E4 system (Q-Sense Inc.) and a QCM (Maxtek Inc.). The Maxtek QCM measures changes in the first harmonic frequency and the change in resistance, whereas the QCM-D measures seven different harmonics from the first to the 13th and their corresponding dissipation factors. Both the QCM and QCM-D instruments had a fundamental resonance frequency of 5 MHz. In all experiments, SiO_2-coated quartz crystals were used and cleaned with a plasma etcher device (SPI Supplies, Plasma Prep II) in the presence of oxygen. All measurements were made with the crystals in flow cells where the crystals were in contact with a liquid phase on only one side. For the QCM-D, the -temperature was maintained at 25 (±0.02)°C and, for the QCM, the temperature was maintained at 25 (±0.1)°C. In all experiments, the ionic strength was kept constant at 1.7 mM, the effective ionic strength of a salt-free PCBS solution at 10 mM based on the electrostatic wormlike chain theory. [47] This corresponds to an effective Debye length of 7 nm. For all experiments, 10 alternate layers of PAH and PCBS were adsorbed on the SiO_2-coated quartz crystals. All QCM-D measurements were done in triplicate except for the experiments at 5 mM repeat unit concentration which were done in duplicate. All QCM measurements were done in triplicate except for the experiment at 5 mM repeat unit concentration which was done once. The experimental setup used for the QCM is shown in the Supporting Information.

QCM is an effective tool to understand the process of film formation that gives insight into the compositional properties at the molecular level. It is an ultrasensitive mass sensor, consisting of a piezoelectric quartz crystal sandwiched between a pair of electrodes. When an AC voltage is applied across the electrodes, the quartz crystal oscillates at its resonant frequency. If a rigid layer is evenly deposited on one or both sides of the electrodes, the resonant frequency will decrease proportionally to the mass of the absorbed layer according to the Sauerbrey equation:[48]

$$\Delta f_m = -\frac{2 \times f_0^2 \times \Delta m}{A \times \sqrt{\rho_q \mu_q}} \tag{2}$$

where Δf_m = measured frequency shift, f_0 = fundamental frequency of the crystal, Δm = mass change per unit area, A = piezo-electrically active area, ρ_q = density of quartz (2.648 g/cm^3), and μ_q = shear modulus of quartz (2.947×10^{-11} dyne/cm^2).

Equation 2 is not valid if the deposited mass is (a) not rigidly deposited on the electrode surface, (b) slips on the surface, or (c) is not evenly deposited on the surface of the electrodes. As described by Kanazawa et al.,[49] the resonant frequency of the QCM crystal also depends on the viscosity and density of the gas or liquid which is in contact with the crystal. The change in the resonant frequency of the QCM crystal due to density and viscosity effects is given by

$$\Delta f_{aqueous} = -\left[\frac{n f_0^{3/2}}{(\pi \mu_q \rho_q)^{1/2}}\right](\rho_L \eta_L)^{1/2} \tag{3}$$

in which

n = number of crystal faces in contact with the liquid

ρ_l = density of the bulk liquid

η_l = viscosity of the bulk liquid

In addition to the changes in frequency, QCM-D can also measure the dissipation which is inversely proportional to the decay time, τ, and given by

$$D = \frac{1}{\pi f \tau} \tag{4}$$

in which f is the crystal oscillation frequency. For a soft film, the decay time is small due to increased energy loss, leading to higher value of the dissipation, whereas for a rigid film, the decay time is large leading to smaller values of dissipation. Thus, the change in dissipation (ΔD) can be used to obtain information about the mechanical properties of the films.

Results and Discussion

The alternate adsorption of PAH and PCBS on quartz crystals coated with silica was studied to understand the composition and structural properties of the ISAM films using a combination of QCM-D, absorbance, and ellipsometry measurements. Four different deposition conditions were used, as summarized in Table 1. In the first deposition condition, the concentrations of both PAH and PCBS were 1 mM based on repeat unit and pH 7.0. This is abbreviated as$(PAH\text{-}1/PCBS\text{-}1)_{7/7}$; the number after the polymer designation gives the concentration and the first and second numbers in the subscript give the pHs of PAH and PCBS, respectively. The other three deposition conditions were:$(PAH\text{-}5/PCBS\text{-}5)_{7/7}$,$(PAH\text{-}10/PCBS\text{-}10)_{7/7}$,$(PAH\text{-}10/PCBS\text{-}10)_{9/8}$. The first three deposition conditions (1, 2 and 3 from Table 1) were chosen to probe the effect of concentration of the polyelectrolytes. The third and fourth deposition conditions were used to study the effect of the solution pH which affects the ionization of polyelectrolytes which, in turn, affects the adsorbed polymer chain conformation. When the polymer is highly charged, chains tend to adsorb in flat, train-like conformations whereas, when the polymer is relatively uncharged, chains adsorb with thick and looplike conformations due to decreased repulsion between

(47) Davis, R. M.; Russel, W. B. *Macromolecules* **1987**, *20*, 518–525.

(48) Sauerbrey, G. *Z. Phys.* **1959**, *155*, 206–222.

(49) Kanazawa, K.; Gordan, J. *Anal. Chem.* **1985**, *57*, 1770–1771.

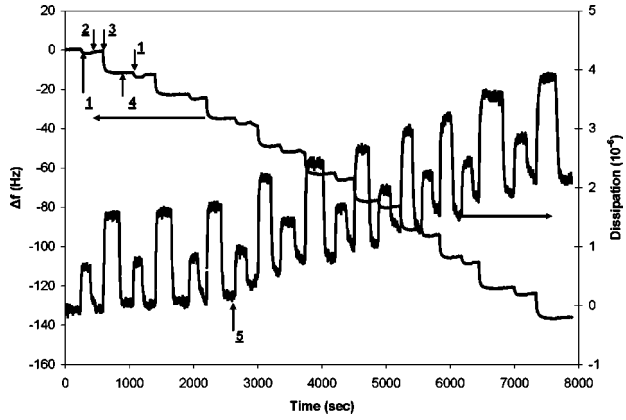

Figure 1. QCM-D results showing changes in the 7th harmonic frequency and dissipation of 10 adsorption cycles of PAH and PCBS for the deposition condition $(PAH\text{-}10/PCBS\text{-}10)_{7/7}$ at an effective ionic strength $I_{eff} = 1.7$ mM and at 25 °C. The flow rate was maintained at 0.3 mL/min throughout the experiment. Arrow "1" marks the injection of PAH followed by rinsing with DI water shown by the arrow marked "2". The PCBS deposition and rinsing steps are shown by arrows marked "3" and "4", respectively. Arrow "5" indicates the beginning of the 4th bilayer.

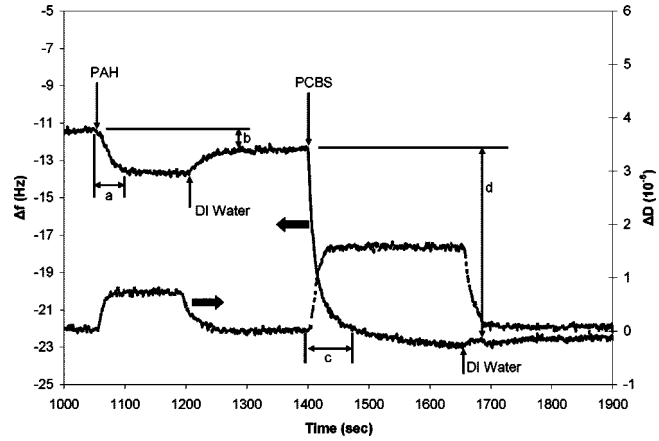

Figure 2. Enlarged section from Figure 1 for the second bilayer of PAH and PCBS. The PAH and PCBS adsorption and rinsing steps are shown by arrows. "a" and "c" denote the times for PAH and PCBS to reach complete adsorption, respectively. "b" and "d" denote the shift in frequency for the PAH and PCBS adsorption steps, respectively. The data shown are normalized from the 7th harmonic.

the chains.[8,9,50,51] Because the pK_a of PAH is 8.7,[52] it was expected that the PAH layers would be thicker in deposition condition 4 compared to conditions 1, 2, and 3.

The QCM-D results for 10 alternate adsorption cycles of PAH and PCBS on silica coated quartz crystal for the condition $(PAH\text{-}10/PCBS\text{-}10)_{7/7}$ are shown in Figure 1. Except for the first harmonic and, in very few cases, the third harmonic, which had high noise levels, the higher harmonics overlapped each other and led to the same final results for film properties (see Supporting Information for the analysis of the films' viscoelasticity). Thus, all results shown here involve normalized changes in the frequency for the seventh harmonic versus time and the corresponding changes in dissipation. The normalization is done by dividing the change in frequency by its harmonic number. In Figure 1, a baseline was first obtained with DI water and then PAH was injected as shown by the arrow marked "1". Upon introducing PAH, a drop in frequency was seen which reached a plateau in ~60 s, indicating complete adsorption. After PAH adsorption was complete, DI water was injected as shown by the arrow marked "2" to rinse the loosely bound polyelectrolyte from the surface; this leads to an increase in frequency. The change in frequency could be due to adsorption or to the effect of bulk properties of the fluid.[49] However, comparing the baseline when the silica coated quartz crystal was in contact with DI water before and after an adsorption step eliminated the effect due to bulk properties of the solution and thus the changes in frequency reflected only the mass uptake by the QCM-D. The adsorption and rinsing steps were repeated for PCBS as shown by arrows marked "3" and "4" respectively. This entire process was repeated for 10 bilayers of PAH and PCBS. The frequency shifted linearly with the number of bilayers, indicating a homogeneous growth of these films. However, linear growth in dissipation was observed only after deposition of 3 bilayers with the slope of the dissipation much less up to 3 bilayers as compared to the slope thereafter. This is possibly due to the effect of the underlying rigid silica layer. A similar interfacial effect due to the underlying gold surface was observed by Caruso et al.;[21] a linear growth in the change in frequency only after 2 bilayers of PAH/PSS adsorption was observed.

Figure 2 shows the enlarged section of the second adsorption step of PAH and PCBS for the results shown in Figure 1. Timelines "a" and "c" indicate the time for almost complete adsorption (>90% complete adsorption) of PAH and PCBS which is on the order of one minute. The frequency shift for PCBS adsorption, indicated by "d" is much higher as compared to PAH adsorption, indicated by "b", indicating that a higher mass of PCBS is adsorbed for every bilayer of PAH and PCBS. A quantitative estimation of molar ratio of PCBS to PAH adsorbed in the films at different polymer concentrations and pH is shown in a later section. The change in ΔD when it is in contact with the polyelectrolyte solutions—either PAH or PCBS—is larger than when the same films are in contact with DI water. This could be due to the viscosity and density of the polyelectrolyte solutions[49] with which the crystal is in contact as well as due to the presence of loosely bound chains that are ultimately rinsed off with DI water, making the films rigid which in turn leads to a decreased dissipation value. Observing the trends in Δf and ΔD when switching from one solution to another can help to understand whether the adsorption kinetics are affected by the viscosity and density of the liquid phase. For example, for the PCBS curve in Figure 2, there is a negligible change in Δf just before rinsing with DI water compared to after rinsing, whereas there is a noticeable change in ΔD, $\sim 1.5 \times 10^{-6}$. In view of the effect of liquid phase viscosity and density on Δf as described by eq 3, we conclude that viscosity and density effects are relatively insignificant for these deposition conditions. Thus, the observed change in ΔD is most likely due to loosely bound PCBS chains that are rinsed away.

The kinetics of polyelectrolyte deposition shown in Figure 2 are summarized in Table 2 in terms of the time required for 95% complete adsorption for PAH and PCBS. The deposition kinetics were fitted to a single exponential function from which the decay time τ_d was estimated. The time required for 95% completion of deposition is then $3\tau_d$. The Reynolds Number, Re, ranged between 0.96−1.61 based on the hydraulic diameter of the flow cell as the characteristic length which, in this case, was 1.2 mm. In all cases, deposition of both PCBS and PAH as well as the DI water rinsing step appeared to be 95% complete within about 60 s, which is relevant for ISAM film formation, particularly for films involving a large number of bilayers. By comparison, an earlier study of deposition kinetics of PCBS and PDDA, done

(50) Burke, S. E.; Barrett, C. J. *Langmuir* **2003**, *19*, 3297–3303.
(51) Stuart, M. A. C.; Hoogendam, C. W.; Keizer, A.d *J. Phys.: Condens. Matter* **1997**, *9*, 7767–7783.
(52) Fang, M.; Kim, C. H.; Saupe, G. B.; Kim, H.-N.; Waraksa, C. C.; Miwa, T.; Fujishima, A.; Mallouk, T. E. *Chem. Mater.* **1999**, *11*, 1526–1532.

Table 2. Kinetics of Polymer Adsorption Showing the Time Required to Reach 95% Complete Adsorption As a Function of Flow Rate and Reynolds Number at Different Deposition Conditions[a]

condition	flow rate (mL/min)	Reynolds number, Re	time required for 95% complete adsorption, s	
			PAH	PCBS
1 $(PAH\text{-}1/PCBS\text{-}1)_{7/7}$	0.40	1.28	39 ± 1	40 ± 6
2 $(PAH\text{-}5/PCBS\text{-}5)_{7/7}$	0.30	0.96	62 ± 4	53 ± 0.3
3 $(PAH\text{-}10/PCBS\text{-}10)_{7/7}$	0.30	0.96	64 ± 4	55 ± 3
4 $(PAH\text{-}10/PCBS\text{-}10)_{9/8}$	0.50	1.61	29 ± 3	39 ± 2

[a] The standard deviations are reported.

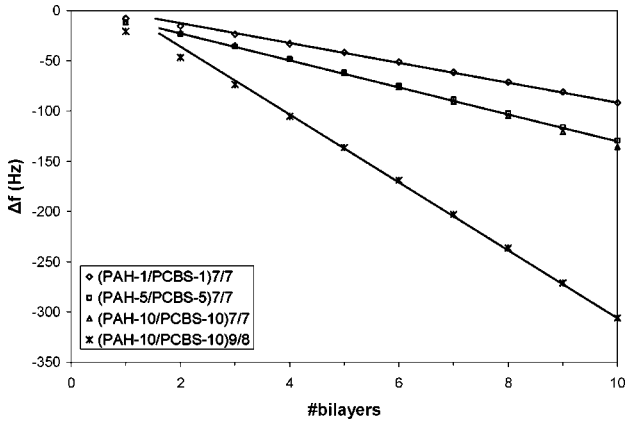

Figure 3. Change in frequency Δf from QCM-D with the number of bilayers for different deposition conditions as indicated in Table 1. For all cases, the effective ionic strength $I_{eff} = 1.7$ mM and temperature was maintained at 25 °C. The slopes were calculated for bilayer no. > 3 and are listed in Table 2. The lines are drawn as a guide to the eye.

with a QCM under static conditions and comparable polymer concentrations and pH conditions as in the present study, showed deposition was 95% complete within 5−6 min. [18] The more rapid deposition kinetics we've observed are due to the effects of convection. It is intriguing to note the marked decrease in both the PCBS and PAH adsorption times for the deposition condition $(PAH\text{-}10/PCBS\text{-}10)_{9/8}$ compared to the $(PAH\text{-}10/PCBS\text{-}10)_{7/7}$ condition. This could be due to the increased pH, especially for the PAH step, as well as to the increased flow rate. In a related study of multilayer growth of PAH/PCBS films, Mermut and Barrett found that the kinetics of bilayer thickness growth under static conditions—measured ex-situ using ellipsometry—accelerated greatly at pH 9 where the charge density of PAH was reduced.[8] For PAH/PCBS concentrations of 10 mM, their films showed no increase in thickness per bilayer after a deposition time of 60 s which is consistent with our observation of the kinetics. A more detailed study of adsorption kinetics is currently underway to probe the separate effects of deposition pH, flow rate, and polymer concentration.

Effect of Concentration and pH on Film Composition. The frequency change Δf versus number of bilayers for the various deposition conditions listed in Table 1 are shown in Figure 3. A linear change in Δf with number of bilayers was observed for all deposition conditions. To avoid the effect of the rigid SiO_2 layer on film properties, the slopes of Δf versus the number of bilayers were calculated after three bilayers were deposited (Table 3). The films for the condition $(PAH\text{-}10/PCBS\text{-}10)_{7/7}$ showed a linear increase in absorbance and thickness up to 600 bilayers in a previous study.[20]

The effect of polymer concentration on frequency change is illustrated in Figure 4 in which the first harmonic data from QCM and the seventh harmonic normalized with the overtone number from the QCM-D are shown. The experimental data from QCM-D and QCM are in good agreement. To our knowledge, this is the first time such a direct comparison has been made between a QCM and QCM-D for polyelectrolyte LbL films. The frequency change $(-\Delta f)$ per bilayer increased with the concentration from 1 to 5 mM of PAH and PCBS, whereas there was little change when the concentration of polyelectrolytes increased from 5 to 10 mM. This suggests a saturation limit for polymer adsorption rather like an adsorption isotherm plateau.

Table 3. Change in Frequency $(-\Delta f)$ Per Bilayer for PAH and PCBS and Change in Frequency for Individual Layers of PAH and PCBS Averaged over Bilayer Numbers 4−10[a]

deposition condition	$-\Delta f$ per bilayer	$-\Delta f_{PAH}$ per bilayer	$-\Delta f_{PCBS}$ per bilayer
1 $(PAH\text{-}1/PCBS\text{-}1)_{7/7}$	9.6 (±0.2)	1.1 (±0.3)	8.2 (±0.6)
2 $(PAH\text{-}5/PCBS\text{-}5)_{7/7}$	13.7 (±0.2)	2.6 (±0.4)	10.5 (±0.7)
3 $(PAH\text{-}10/PCBS\text{-}10)_{7/7}$	14.1 (±0.4)	2.7 (±0.4)	11.4 (±0.8)
4 $(PAH\text{-}10/PCBS\text{-}10)_{9/8}$	33.9 (±0.7)	9.6 (±0.8)	24.1 (±1.6)

[a] The standard deviations are reported.

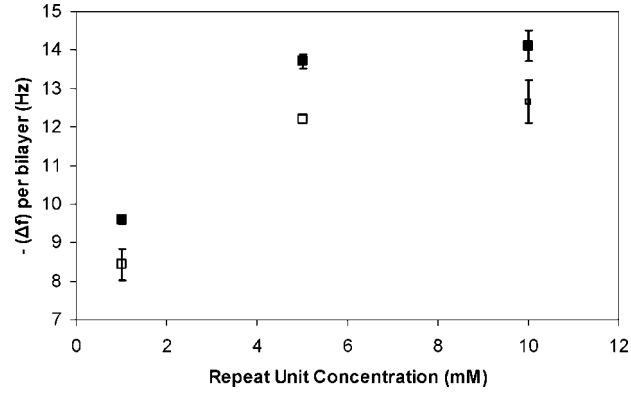

Figure 4. Change in frequency $(-\Delta f)$ per bilayer as a function of polymer concentration for QCM-D [filled squares] and QCM [open squares]. Results are shown for three different deposition conditions: $(PAH\text{-}1/PCBS\text{-}1)_{7/7}$, $(PAH\text{-}5/PCBS\text{-}5)_{7/7}$, $(PAH\text{-}10/PCBS\text{-}10)_{7/7}$; the experiments were done at constant ionic strength of $I_{eff} = 1.7$ mM and 25 °C. The slopes are based on the data for >3 bilayers to avoid quartz substrate effects. The error bars represent ±1 standard deviation.

The repeat unit molar ratio M_{PCBS}/M_{PAH} in a film can be estimated from the Δf data for the individual PAH and PCBS deposition steps from the QCM-D experiments by

$$\frac{M_{PCBS}}{M_{PAH}} = \frac{\Delta f_{PCBS}/MW_{PCBS}}{\Delta f_{PAH}/MW_{PAH}} \quad (5)$$

in which MW_{PCBS} and MW_{PAH} are the repeat unit molecular weights of PCBS and PAH, respectively. In eq 5, the frequency changes for PAH and PCBS were estimated using the frequency shifts marked by "b" and "d", respectively, in Figure 2. To calculate M_{PCBS}/M_{PAH}, it was assumed that the PAH and PCBS monolayers have the same water content, i.e., the same hydration level. Since both PAH and PCBS have one ionic group in their repeat units, the molar ratio in which they adsorb can give a quantitative measurement of percent dissociation of these films upon adsorption of one polyelectrolyte on the other.

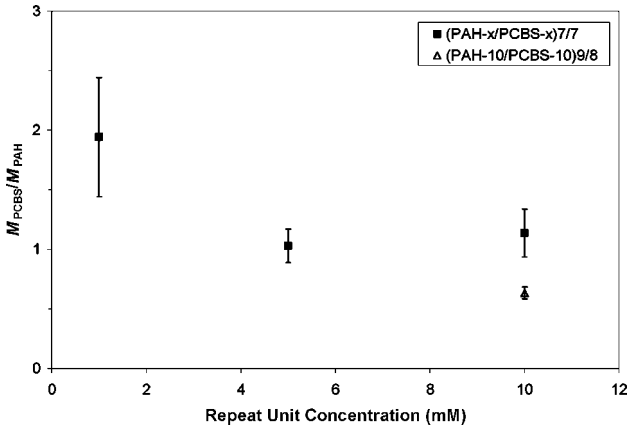

Figure 5. Repeat unit molar ratio of PCBS to PAH from eq 5 as a function of polymer concentration while varying pH at constant ionic strength I_{eff} = 1.7 mM and 25 °C. Filled squares refer to pH of 7/7 at three different concentrations and the open triangle refers to the pH condition of 9/8. "*x*" in the legend refers to the repeat unit concentration of both polymers.

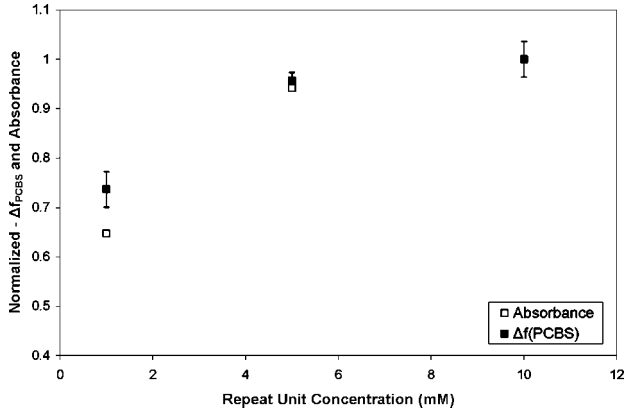

Figure 6. Comparison of total PCBS in ISAM films obtained from QCM-D compared to the absorbance data obtained from equivalent films deposited on glass slides at PAH/PCBS pH values of 7/7. The absorbance data were measured at 360 nm in the dry state whereas Δf_{PCBS} was measured for the hydrated films (Table 3).

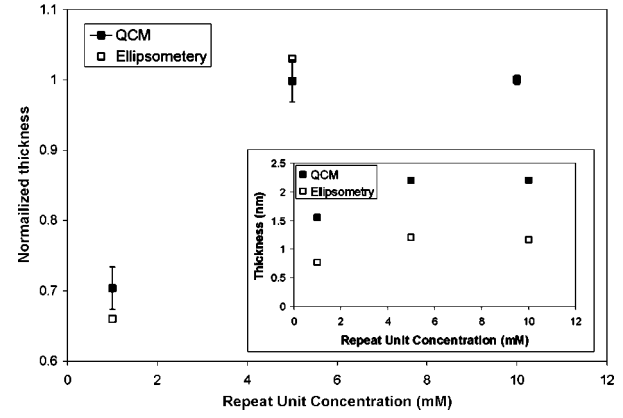

Figure 7. Normalized thicknesses obtained from QCM-D and ellipsometry measurements for PAH and PCBS deposited at different repeat unit concentrations and at PAH/PCBS pH values of 7/7, a constant ionic strength I_{eff} = 1.7 mM, and at 25 °C. The inset shows the absolute values of thickness per bilayer obtained from the two techniques.

Values of the molar ratio M_{PCBS}/M_{PAH} are plotted against the repeat unit concentration in Figure 5. M_{PCBS}/M_{PAH} is close to 1 at 5 and 10 mM polymer concentrations at pH 7 where prior work has shown that these polyelectrolytes are almost fully ionized.[8] A similar result was observed by Lvov et al. for the alternate adsorption of poly(styrene sulfonate) (PSS) and poly(ethyleneimine) (PEI), which using a QCM, were found to adsorb at a 1:1 molar ratio.[43] The value $M_{PCBS}/M_{PAH} \sim 2$ calculated at 1 mM concentration was unexpectedly high and may be due to the relatively high standard deviation in the measurement of Δf_{PAH}, since the adsorbed amount was so small. For the condition (PAH-10/PCBS-10)$_{9/8}$, $M_{PCBS}/M_{PAH} \approx 0.63$, which is likely due to the deposition of PAH in thick, looplike layers since the pK_a of PAH is 8.7, which leads to reduced charge repulsion on the polymer chain.[52] The increased adsorption of PAH leads, in turn, to an increased adsorption of PCBS, shown later in Table 4. However, the relative amount of increased PCBS adsorption is small compared to PAH since PCBS is adsorbed at pH 8.0 which is far above its pK_a (~3.3)[53] and hence the PCBS chains are highly charged and tend to absorb in flat train-like conformations.[54] This is evident from Table 3 which shows an increase in PAH adsorption of almost 3.2 times from neutral pH conditions as compared to a 2-fold increase for PCBS.

Previous studies of ISAM film fabrication have shown that film thickness does not always increase linearly with bilayer number. In some cases, nonlinear film growth, particularly exponential growth, has been observed. Nonlinear film growth has been attributed to poor solvent quality,[46] to insufficient rinsing times,[20] and to the diffusion of polyelectrolytes out of the ISAM film.[38] The effect of the degree of charge (DC) of the polymer on formation of polyelectrolyte multilayers has been previously reported; it was found that a minimum DC is a required for formation of stable polymer multilayer films. In studies by Steitz et al.[55,56] and by Voigt et al.,[55,56] the DC of a random copolymer of cationic DADMAC monomers and neutral NMVA monomers, poly(diallyl-dimethyl-ammoniumchloride *stat-N*-methyl-*N*-vinylacetamide), was varied while forming multilayers with the sodium salt of poly(styrene sulfonate)(PSS). It was found that a minimum DC of 68% was needed for the formation of stable multilayer films. It was proposed that the 68% threshold was related to a threshold of charge reversal necessary for formation of a multilayer system. In our work, the molar ratio M_{PCBS}/M_{PAH} ~1 for the deposition condition (PAH-10/PCBS-10)$_{7/7}$ where both PAH and PCBS are fully charged. We believe this is the reason for the formation of stable, optically homogeneous multilayers observed for up to at least 600 bilayers in our earlier study.[20] By contrast, a molar ratio $M_{PCBS}/M_{PAH} \sim 0.63$ for the deposition condition (PAH-10/PCBS-10)$_{9/8}$, where the DC for PAH is less than 1 may explain the observed lack of stable film formation for more than 200 bilayers due to a possible charge imbalance. Thus, it seems that a molar ratio of close to 1 or complete dissociation of ionic groups may be one of the requirements for linear growth of ISAM films, especially at high bilayer numbers.

The data obtained from QCM-D experiments in the wet state were compared with absorbance measured for the dry films. The absorbance measurements at 360 nm track the deposition of PCBS as a function of concentration since PAH does not absorb at this wavelength. The frequency shift for PCBS, Δf_{PCBS}, was compared to the absorbance measurements at 360 nm at different deposition concentrations (Figure 6). Both frequency shift and absorbance data were normalized with respect to the absorbance

(53) Rmaile, H. H.; Schlenoff, J. B. *Langmuir* **2002**, *18*, 8263–8265.
(54) Steeg, H. G. M. v. d.; Stuart, M. A. C.; Keizer, A. d.; Bijsterbosch, B. H *Langmuir* **1992**, *8*, 2538–2546.
(55) Steitz, R.; Jaeger, W.; Klitzing, R.v *Langmuir* **2001**, *17*, 4471–4474.
(56) Voigt, U.; Jaeger, W.; Findenegg, G. H.; Klitzing, R. V. *J. Phys. Chem. B* **2003**, *107*, 5273–5280.

Table 4. Water of Hydration and Chromophore Density Estimated Using a Combination of QCM-D and Ellipsometry Data for Different Deposition Conditions (Refer to Table 1)[a]

deposition condition	PCBS (mg/m^2) dry	thickness per bilayer (nm) QCM-D	thickness per bilayer (nm) Ellipsometry	water content[b] (%)	*N*, no. of PCBS chromophores(cm^{-3})
1 (PAH-1/PCBS-1)$_{7/7}$	0.81	1.55 (±0.02)	0.77 (±0.04)	45.8	1.7×10^{21}
2 (PAH-5/PCBS-5)$_{7/7}$	1.15	2.20 (±0.02)	1.20 (±0.04)	40.5	1.6×10^{21}
3 (PAH-10/PCBS-10)$_{7/7}$	1.14	2.20 (±0.01)	1.16 (±0.01)	42.5	1.6×10^{21}
4 (PAH-10/PCBS-10)$_{9/8}$	2.21	5.16 (±0.04)	2.75 (±0.09)	41.8	1.4×10^{21}

[a] The standard deviations are reported. [b] The water content was calculated using eq 7.

and Δf_{PCBS} at 10 mM to compare results from these different experiments. The absorbance of these films depends not only on the concentration of the PCBS chromophores, but also on the local chemical environment and the orientation of the chromophores. However, for this comparison, it was assumed that the extinction coefficient of these films was not a function of deposition concentration at deposition pH values of 7/7, i.e., the deposition conditions 1−3 in Table 1. The fact that the QCM-D data track the absorbance results so well supports the validity of the QCM-D analysis. The comparison of absorbance for deposition condition 4, i.e., (PAH-10/PCBS-10)$_{9/8}$, was not made, since the extinction coefficient could vary significantly from neutral pH conditions to elevated pH conditions.

Voigt Model Analysis of Films. The thicknesses of the wet films were calculated by fitting the frequency and dissipation data with the Voigt model which is based on a spring and dashpot connected in parallel.[33,34,57] This model is one of several that can be used to estimate the thickness and mechanical properties, such as the viscosity and shear modulus of the adsorbed films (see Supporting Information). By utilizing data for changes in frequency as well as changes in dissipation, the Voigt model can be used when the Sauerbrey equation, Eq. 2, is not valid. To calculate the hydrated film thickness t_h from the Voigt model (see eqs 10 and 11 in Supporting Information), it is necessary to specify a value for the density of the hydrated polymer film, ρ_h. Since there was no independent measurement of ρ_h, a value of ρ_h was initially assumed and then the hydrated film thickness t_h was calculated. The hydrated film density was then recalculated from the equation:

$$\rho_h = \frac{\rho_d t_d + \rho_w (t_h - t_d)}{t_h} \tag{6}$$

in which it was assumed that the hydrated film was a combination of a dry film with thickness t_d (measured by ellipsometry) and a layer of coupled water with thickness$(t_h - t_d)$ and where ρ_d is the density of a dry polyion film (1200 (±100) kg/m^3[3,21,43]), and ρ_w is the density of water. The value of ρ_h calculated from eq 6 was then used in the Voigt model to recalculate t_h in an iterative fashion until successive values of ρ_h agreed to within ±1%. Using this approach, ρ_h was found to be 1100 kg/m^3 and this was the value used to calculate the hydrated film thicknesses shown in Figure 7 and Table 4.

From both QCM-D and ellipsometry, film thicknesses increased with the PAH and PCBS concentrations from 1 to 5 mM, but did not change much upon increasing the concentration to 10 mM. The QCM-D analysis led to thicknesses about 2X greater than those from the dry films that were measured by ellipsometry(inset in Figure 7). The water content in these films is listed in Table 4 and was estimated by

$$\%\ \text{Water Content} = \frac{\rho_h t_h - \rho_d t_d}{\rho_h t_h} \cdot 100 \tag{7}$$

The water content was estimated to vary between 41−46% which is comparable to ∼50% water content for ISAM films comprised of PAH and PSS studied by Ramsden et al. using a polar optical waveguide as the deposition substrate.[58] As an additional check on these calculations, the water content was calculated using the Sauerbrey equation in which the Δf per bilayer was converted to the mass deposited per unit area for wet films (m_w). The mass per unit area for dry films (m_d) was calculated by multiplying the thickness of dry films, which was calculated using ellipsometry with the assumed density of the dry films (1200 ± 100 kg/m^3). The % water content was calculated by using the equation: % water content = $[(m_w - m_d)/m_w] \times 100$. The values obtained by this procedure and the procedure described above were found to agree to within 2−5% (see Table S1 in Supporting Information). Thus, in all cases in the present study, the water content calculated from the Voigt model agreed well with that calculated from the Sauerbrey equation.

General criteria showing when the Sauerbrey equation can be used and when a more general viscoelasticity model is needed were derived by White and Schrag by considering a viscoelastic film (phase 1) with thickness t_h, viscosity η_1 and density ρ_1 on a quartz crystal surface in contact with a liquid (phase 2) with viscosity η_2 and density ρ_2.[59] The Sauerbrey equation and a more generalized viscoelastic model were shown to diverge when $\beta_1 t_h > 0.28$ and when $\beta_1/\beta_2 < 0.2$ where β_i is defined as

$$\beta_i = \sqrt{\frac{\omega \rho_i}{\eta_i}} cos\left[\frac{\pi}{4} - \frac{\varphi}{2}\right] \tag{8}$$

in which ϕ is the relative phase angle of the medium. For a purely viscous medium, $\phi = \pi/2$, whereas $\phi = 0$ for a purely elastic medium. These criteria were found to explain the swelling behavior of films of ammonium poly(4-styrenesulfonic acid) studied with a QCM-D.[35]

In the present study, exact values for viscosity of the films could not be calculated using the Voigt model because the fitted values of the viscosity and shear modulus had unacceptably high standard deviations. The net increase in dissipation after adsorption of one bilayer of PAH and PCBS was small, indicating that the films were relatively rigid. For example, for the deposition condition (PAH-10/PCBS-10)$_{9/8}$, we observed a maximum dissipation increase $\Delta D = 0.2 \times 10^{-6}$ for every 10 Hz change in frequency and found that the Sauerbrey equation and the Voigt model gave similar results. For these films with $t_h = 52$ nm and $\rho_h = 1100$ kg/m^3, we calculated a range of values for $\beta_1 t_h$ using eq 8 with limiting values of the film viscosity since exact values were not known. Values of $\beta_1 t_h$ were calculated to be 0.003 and 0.22 assuming that the films behaved like purely elastic materials ($\eta \approx 10$ Pa s; $\phi = 0$) and purely viscous materials ($\eta = 10^{-3}$ Pa s; $\phi = \pi/2$), respectively. Both limiting cases satisfied the criterion $\beta_1 t_h < 0.28$ where the Sauerbrey equation and the Voigt model would converge. For the second criterion involving the ratio β_1/β_2, values were calculated to be 0.01 (purely elastic) and 0.75 (purely viscous). The ratio for the purely viscous case does not satisfy the criterion of <0.2 for the Sauerbrey equation to apply because the assumed film viscosity in this limit was taken to be that of water. Since these films are actually semidilute,

ionically cross-linked polymer gels, the actual film viscosity is certainly several-fold greater than that of water.

The criteria of White and Schrag also are consistent with a QCM-D study of collagen films adsorbed on polystyrene in which $\Delta D = 1.7 \times 10^{-6}$ for every 10 Hz change in frequency was observed and the Sauerbrey equation was found not to apply.[60] Using values of film viscosity, shear modulus, and thickness from the Voigt model with an assumed range of film densities, values of $\beta_1 t_h$ were 0.38 and 0.61 while values of β_1/β_2 were 0.41 and 0.38 for thicknesses of 170 and 130 nm, respectively. In another study of ISAM films consisting of PAH and a polyanionic mixture of poly(L-glutamic acid) (PGA) and PSS, the Sauerbrey equation was found to accurately describe the film thickness for $\Delta D \sim 0.014 \times 10^{-6}$ for every 10 Hz change in frequency.[38] This corresponds well to the supposition that, although there is a positive shift in the dissipation which theoretically should invalidate the Sauerbrey equation, the Sauerbrey equation can still be valid experimentally for low changes in dissipation.

The change in frequency for PCBS, Δf_{PCBS}, and PAH, Δf_{PAH}, as shown in Table 3 can be converted to *%PCBS* (weight %) in these films which, together with the density of the film in the dry state, can be used to estimate the number density of PCBS chromophores, *N* (see eq 1) using

$$N = \frac{\%PCBS \times \rho_d \times N_{av}}{100 MW_{PCBS}} \quad (9)$$

where N_{av} is Avogadro's number.

Table 4 shows the calculated values of *N* which are in the range of $1.4-1.7 \times 10^{21}$ cm^{-3}. By comparison, for poled polymer films, an alternative approach for making second order nonlinear optical films, values of *N* have been reported ranging from 2.2 to 9.8×10^{20} cm^{-3}.[61,62]

Using the Voigt model and the procedure described above, the hydrated film thickness per bilayer for deposition condition 4 (PAH-10/PCBS-10)$_{9/8}$ was calculated to be 5.16 nm, a value 2.3 times higher than that observed for the neutral pH condition-(deposition condition 3). By comparison, the dry film thickness obtained from ellipsometry for deposition condition 4 was 2.4 times higher than that for condition 3. The observed increase in the bilayer film thickness with the PCBS concentration for highly charged PAH (Figure 7 for deposition conditions 1−3) is also consistent with the findings of Voigt et al.[56] who found that, for the degree of charge DC > 75%, the thickness of stable multilayer films increased with polymer concentration.

Conclusions

The alternate adsorption of polycation poly(allylamine hydrochloride)(PAH) and the polymeric dye poly1{[-*p*-(3′-carboxy-4′-hydroxyphenylazo)benzenesulfonamido-1,2-ethandiyl]} (PCBS) on quartz crystals coated with silica was studied to understand the film structure and adsorption kinetics using a combination of quartz crystal microbalance with dissipation monitoring(QCM-D), QCM, absorbance, and ellipsometry measurements. The effects of polymer concentration and pH on the structural properties of these films were studied. For adsorption from pH 7, there was a significant increase in the mass adsorbed when the polymer concentration was increased from 1 to 5 mM. However, the mass adsorbed remained essentially the same when the concentration was increased from 5 to 10 mM, akin to the saturation of an adsorption isotherm. At PAH and PCBS concentrations of 5−10 mM, the polymers adsorbed in a molar ratio of 1, implying a complete dissociation of ionic groups. The absorbance measurements, which track the amount of PCBS in these films, were found to be in good agreement with the QCM-D results for the PCBS deposition step. In a second set of experiments, the pH of the polymer solutions was increased to study the charge effects on the adsorption behavior of the polymers. Higher values of pH resulted in increased mass adsorbed for PAH due to reduced charge density on the polymer chains, which favored the deposition of polymer in loops and tails. A higher mass of PAH adsorbed, in turn, led to an increased adsorption of PCBS. The molar ratio of PCBS to PAH at pH of 8 and 9, respectively, was found to be 0.63. By comparing these results with recent nonlinear optical work by our group, it is believed that the molar ratios in which the polymers adsorb might play a role in the polar ordering of chromophores in films. The normalized thicknesses obtained by the QCM-D results for the hydrated films were found to be in good agreement with thicknesses for the corresponding dry films obtained from ellipsometry. By comparing the thickness obtained by the QCM experiments with the thickness obtained by ellipsometry, the water content in these films was found to be in the range of 41−46% by weight.

The combination of QCM-D results with ellipsometry and absorbance data indicates that QCM-D can be reliably used to study the structural and compositional properties of thin polymer films. A more detailed study on the adsorption kinetics of polyelectrolytes using QCM-D is the subject of a future paper.

Acknowledgment. The authors thank Q-Sense Inc. and Maxtek Inc. for their technical support. The authors also thank the following for financial support: NSF Grant No. ECS-0524625, the Macromolecules and Interfaces Institute at Virginia Tech for a fellowship for AG, and Luna Innovations (Subcontract No. 1194-RM-2S/VT), and the Institute for Critical Technology and Applied Science at Virginia Tech.

Supporting Information Available: Details of ellipsometry and the experimental setup for QCM; QCM-D data for ISAM film formation using the fifth, seventh, ninth, eleventh, and thirteenth harmonics; a brief introduction to the Voigt model and a comparison of the film thicknesses calculated from the Voigt model and Sauerbrey equation; and a comparison of the %water content in these films obtained using Voigt model and Sauerbrey equation. This material is available free of charge via the Internet at http://pubs.acs.org.

LA8005053

(57) Ferry, J. D. *Viscoelastic properties of polymers*; 3rd ed.; John Wiley and Sons, Inc.: New York, 1980.
(58) Ramsden, J. J.; Lvov, Y. M.; Decher, G. *Thin Solid Films* **1995**, *254*, 246–251.
(59) White, C. C.; Schrag, J. L. *J. Phys. Chem.* **1999**, *111*, 11192–11206.
(60) Gurdak, E.; Dupont-Gillain, C. C.; Booth, J.; Roberts, C. J.; Rouxhet, P. G. *Langmuir* **2005**, *21*, 10684–10692.
(61) Kim, T.-D.; Kang, J.-W.; Luo, J.; Jang, S.-H.; Ka, J.-W.; Tucker, N.; Benedict, J. B.; Dalton, L. R.; Gray, T.; Overney, R. M.; Park, D. H.; Herman, W. N.; Jen, A. K.-Y. *J. Am. Chem. Soc.* **2007**, *129*, 488–489.
(62) Mortazavi, M. A.; Knoesen, A.; Kowel, S. T.; Henry, R. A.; Hoover, J. M.; Lindsay, G. A. *Appl. Phys. B: Laser Opt.* **1991**, *53*, 287–295.